Proximity effect in superconducting layered structures

J. Z. Wu, X. X. Yao,* C. S. Ting, and W. K. Chu
Department of Physics, University of Houston, Houston, Texas 77204
(Received 4 May 1992)

A general formalism for discussing the superconducting proximity effect and the charge-carrier transfer effect in an inhomogeneous layered structure has been obtained from the Gor'kov equation. Two practical systems, which are finite superconductor/nonsuperconductor multilayer and superlattice, are considered. The physical properties such as the transition temperature, the coherence length, the proximity effect, and the charge-carrier transfer effect have been discussed. When compared with experiment, our calculations show that the depression of the transition temperature in the *c*-oriented Y-Ba-Cu-O/Pr-Ba-Cu-O superlattices is dominantly induced by the proximity effect.

I. INTRODUCTION

It has been an important issue to understand the superconducting properties in a layered structure especially since the discovery of the high-T_c superconductors. A common feature of these materials is the presence of the Cu-O planes, in which reside the charge carriers contributing to the superconductivity. Experiments have revealed a strong anisotropy between the in-plane and the off-plane directions in their physical properties such as the normal-state resistivity and the transport critical current,[1,2] the upper critical field,[3] the thermal conductivity,[4] etc. This suggests a weakly coupled layered structure for the high-T_c superconductors (HTS's).

Recently, with significant progress on the device applications of HTS's materials, this issue becomes even more important. The *c*-oriented $YBa_2Cu_3O_{7-\delta}/RBa_2Cu_3O_{7-\delta}$ superlattices [R =Pr(Ref. 5), Dy (Ref. 6), and Gd (Ref. 7)], which have been used for investigating the interlayer coupling of $YBa_2Cu_3O_{7-\delta}$, are fabricated by epitaxially depositing $YBa_2Cu_3O_{7-\delta}$ and $RBa_2Cu_3O_{7-\delta}$ alternatively along the *c* axis. In a similar way, various *SIS* and *SNS* (Refs. 8 and 9) structures have been reported, showing interesting properties such as the Sharpiro step, the modulation of the junction critical current by the applied magnetic field, etc. The growth of an ultrathin $YBa_2Cu_3O_{7-\delta}$ as a charge supply layer on MgO (Ref. 10) and $SrTiO_3$ (Refs. 11 and 12) has resulted in a field effect device. Basically, all these devices can be described as a kind of inhomogeneous layered structure composed of the Cu-O planes from $YBa_2Cu_3O_{7-\delta}$ and $RBaCu_3O_{7-\delta}$ and the (001) unit-cell planes from MgO, $SrTiO_3$, and other insulating materials.

However, a theoretical understanding of the superconductivity in layered-structure superconductors has not been achieved because the following questions are not answered yet. First of all, the pairing mechanism is not known for high-T_c superconductors even though many models have been proposed. Second, it is not clear how anisotropic the interlayer and the intralayer pair couplings could be. Third, the Gor'kov equation has not been solved for an inhomogeneous system even if one assumes the BCS superconducting mechanism for Y-Ba-Cu-O. Only a few simplified cases, such as the double layers and homogeneous infinite layers, have been discussed.[13–15]

In this paper, we would like to report our work on understanding the superconducting properties of an inhomogeneous layered structure on the basis of the Gor'kov equation. We simplify those multilayers and devices as sets of two-dimensional (2D) planes. The electronic properties of each plane could be very different depending on what material it represents. For HTS's, the charge carriers may form 2D Cooper pairs in the superconducting state. The hopping of the charge carriers between layers may result in the proximity effect. The rest of the paper is organized as follows: Section II contains the description and the full solution of the equations. Two practical systems are going to be discussed. One is the finite multilayers and the other is S/N superlattice. Here we will use S to represent the superconductor and N for normal materials, which includes metals (M), insulators (I), and semiconductors (Sm) or even another superconductor (S). In Sec. III, we will calculate the transition temperature of the S_1/S_2 and S/Sm superlattices, the proximity effect in a SN interface, the coherence length ξ_s and the Cooper-pair penetration length ξ_N in the normal side. In our previous paper,[16] we point out that the proximity effects are mainly responsible for the depression of the superconducting transition temperature in Y-Ba-Cu-O/Pr-Ba-Cu-O superlattices based on the good agreement between our calculated T_c and the experimental data. A pronounced experimental investigation of this issue has been reported[17] recently which excluded the possibility of the dominant role of interdiffusion and charge-carrier transfer and then suggested the role of the proximity effect. Section IV contains discussions and conclusions.

II. FORMALISM

Our system is composed of N two-dimensional planes which correspond to the Cu-O planes for high-T_c copper oxides such as $YBa_2Cu_3O_7$ Bi compounds, Tl compounds, etc., and even the insulating material Pr-Ba-Cu-O. For

$SrTiO_3$, $LaAlO_3$, and some other Porovski structure materials, which could be possible candidates for the insulating layer in the high-T_c superconducting devices, we may consider them to be a layered structure with its unit cell as a plane. The charge carriers are assumed to reside in these planes and can hop between them. The electronic structure of each plane is determined by the kind of material it represents. The superconductivity mechanism for HTS's is assumed to be BCS-like since their basic features in the superconducting state are similar to the conventional superconductors. However, the pairing is not necessarily phonon-mediated electron-electron interaction. Based on the strong anisotropy between the c axis and the ab plane, we assume the pairing to be limited primarily in the Cu-O planes so that only the intralayer pair coupling will be considered. On the insulating layers such as Pr-Ba-Cu-O we simply assume this pair interaction is zero. Two processes could be important when S and N layers are stacking up layer by layer. The proximity effect is induced when the Cooper pairs hop from S layers to N layers. And the charge-carrier transfer effect may become visible if there is a big difference between the charge-carrier densities of S and N layers. Employing the Nambu representation,[18] the Hamiltonian of the layered system can be written as follows:

$$H=\sum_{l,\mathbf{k}}\xi_l(\mathbf{k})\Psi^+_{l,\mathbf{k}}\hat{\tau}_3\Psi_{l,\mathbf{k}} + \frac{1}{2}\sum_{l,\mathbf{k},\mathbf{k}'}V_{l,\mathbf{k},\mathbf{k}'}(\Psi^+_{l,\mathbf{k}}\hat{\tau}_3\Psi_{l,\mathbf{k}'})(\Psi^+_{l,-\mathbf{k}}\hat{\tau}_3\Psi_{l,-\mathbf{k}'}) + \sum_{l,l',\mathbf{k}}T_{l,l'}\Psi^+_{l,\mathbf{k}}\hat{\tau}_3\Psi_{l',\mathbf{k}}\ , \tag{1}$$

where $\Psi_{l,\mathbf{k}}$ is the field operator and it is defined by the creation and annihilation operators for fermion charge carriers of two-dimensional wave vector $\mathbf{k}$ and the z-component spin ($\uparrow$ or $\downarrow$) in the lth Cu-O plane:

$$\Psi_{l,\mathbf{k}}=\begin{pmatrix} c_{l,\mathbf{k}\uparrow} \\ c^+_{l,-\mathbf{k}\downarrow}\end{pmatrix}\ . \tag{2}$$

$\xi_l(\mathbf{k})\equiv\epsilon_l(\mathbf{k})-\mu_l$. μ_l and $\epsilon_l(\mathbf{k})\equiv k^2/2m_l^*$ are the chemical potential and the kinetic energy of the charge carrier with effective mass m_l^* in the lth Cu-O plane. $V_{l,\mathbf{k},\mathbf{k}'}$, which is negative in S layers and zero in N layers, represents the BCS pair coupling and may originate in nonphonon mechanism. $T_{ll'}$ is the hopping matrix. $\hat{\tau}_1$, $\hat{\tau}_2$, and $\hat{\tau}_3$ are Pauli matrices. The finite-temperature Green's function is then defined as[19]

$$\hat{G}_{ll'}(\mathbf{k},\tau)\equiv-\langle T_\tau\Psi_{l,\mathbf{k}}(\tau)\Psi^+_{l',\mathbf{k}}(0)\rangle\ . \tag{3}$$

It is straightforward to show that the Green's function satisfies the Gor'kov equation based on the mean-field approximation,

$$-\frac{\partial\hat{G}_{l,l'}(\mathbf{k},\tau)}{\partial\tau}=\delta_{ll'}\delta(\tau)+[\xi_l(\mathbf{k})\hat{\tau}_3+\Delta_l(\mathbf{k})\hat{\tau}_1]\hat{G}_{l,l'} + \sum_m T_{l,m}\hat{\tau}_3\hat{G}_{m,l'}(\mathbf{k},\tau)\ . \tag{4}$$

Here the gap function or the order parameter $\Delta_l(\mathbf{k})$ is defined as

$$\Delta_l(\mathbf{k})=-V_l\sum_{\mathbf{k}}F_{l,l}(\mathbf{k},0)\ , \tag{5}$$

and we have used the s-wave approximation for the pair interaction

$$V_{l,\mathbf{k},\mathbf{k}'}=\begin{cases}-V_l, & |\xi_l(\mathbf{k})|<E_f, \text{ in superconductors}\\ 0, & \text{otherwise}\ .\end{cases} \tag{6}$$

$F_{l,l}(\mathbf{k},0)=-\langle T_\tau c_{l,\mathbf{k}\uparrow}c_{l,-\mathbf{k}\downarrow}\rangle$, is the off-diagonal matrix element of $\hat{G}_{l,l}(\mathbf{k},\tau)$ at $\tau=0$. Introducing Matsubara's Fourier transform,[19] Eq. (4) can be reduced to a matrix equation

$$\sum_m\hat{G}_{l,m}(\mathbf{k},\omega_n)\cdot\hat{K}_{m,l'}=\hat{\delta}_{l,l'}\ . \tag{7}$$

Therefore solving the Green's function is equivalent to inverting the matrix $\hat{K}$, where the matrix $\hat{K}$ is defined as

$$\hat{K}_{l,l}\equiv i\omega_n\hat{I}-\xi_l(\mathbf{k})\hat{\tau}_3-\Delta_l\hat{\tau}_1\ , \tag{8}$$

$$\hat{K}_{l,l'}\equiv-T_{ll'}\hat{\tau}_3,\quad l\neq l'\ . \tag{9}$$

$\omega_n\equiv(2n+1)\pi k_BT$ is the Matsubara frequency for fermions. Considering the hopping matrix $T_{l,l'}$ short-ranged, we may assume that only the charge carrier hopping between the nearest-neighbor planes is important. Under this condition, the hopping matrix $\hat{T}_{l,l'}$ becomes

$$\hat{T}_{l,l'}=T_{l,l+1}\delta_{l',l+1}\hat{\tau}_3+T_{l,l-1}\delta_{l',l-1}\hat{\tau}_3\ . \tag{10}$$

Therefore the matrix $\hat{K}_{ll'}$ is actually tridiagonal. The inversion of a tridiagonal matrix has been studied by Dy *et al.*[20] for some special case using the perturbation method. By extending their method, we are able to solve Eq. (7) for a finite multilayer such as a SN junction and a superlattice under periodic boundary condition. In order to make this paper short, the detailed derivation of these solutions is given in Appendix A and the rigorous proof is shown in Appendix B.

A. Solutions

1. *Finite multilayers*

When multilayers are not periodic or periodic but the number of the unit cell is small, we call them finite multilayers. The boundary condition for a finite multilayer is written as

$$T_{1,0}=T_{N,N+1}=0\ . \tag{11}$$

Here N is the total number of the planes in the multilayer. Then the solution for Eq. (7) is

$$\frac{1}{\hat{G}_{l,l}}=\frac{1}{\hat{G}^0_{l,l}}-\hat{\Sigma}^{UB}_l-\hat{\Sigma}^{DB}_l\ , \tag{12}$$

$$\hat{G}_{l,l'}=\hat{G}_{l,l}\prod_{i=l+1}^{i=l'}\hat{T}_{i-1,i}\cdot\hat{U}_i,\quad l<l'\ ,$$
$$\hat{G}_{l,l'}=\hat{G}_{l,l}\prod_{i=l-1}^{i=l'}\hat{T}_{i+1,i}\cdot\hat{D}_i,\quad l>l'\ . \tag{13}$$

$\hat{G}^0_{l,l}$ is defined as

$$\hat{G}^0_{l,l}=\hat{K}^{-1}_{l,l}=-\frac{i\omega_n\hat{I}+\xi_l(\mathbf{k})\hat{\tau}_3+\Delta_l(\mathbf{k})\hat{\tau}_1}{\omega_n^2+\xi_l^2+\Delta_l^2}\ , \quad l=1,2,\ldots,N\ . \tag{14}$$

The self-energies $\hat{\Sigma}^{UB}_l$ and $\hat{\Sigma}^{DB}_l$, which represent contributions to layer l from the charge-carrier hopping through all upper layers ($l'>l$) and all lower layers ($l'<l$), respectively, are defined through the following iterative relations:

$$\hat{\Sigma}^{UB}_l=\hat{T}_{l,l+1}\cdot\{(\hat{G}^0_{l+1,l+1})^{-1}-\hat{\Sigma}^{UB}_{l+1}\}^{-1}\cdot\hat{T}_{l+1,l}\ , \tag{15}$$

$$\hat{\Sigma}^{DB}_l=\hat{T}_{l,l-1}\cdot\{(\hat{G}^0_{l-1,l-1})^{-1}-\hat{\Sigma}^{DB}_{l-1}\}^{-1}\cdot\hat{T}_{l-1,l}\ . \tag{16}$$

The iteration of $\hat{\Sigma}^{UB}_l$ and $\hat{\Sigma}^{DB}_l$ starts from $l=N$ and $l=1$, respectively, as

$$\hat{\Sigma}^{UB}_N=0,\quad \hat{\Sigma}^{DB}_1=0\ , \tag{17}$$

which can be obtained directly from Eq. (11). For simplicity of writing, matrices $\hat{U}_i$ and $\hat{D}_i$, which are defined by Eqs. (A11) and (A12) in Appendix A, have been introduced.

2. *Periodic boundary condition*

For a superlattice, or if the number of the unit cell is large enough, we may apply the periodic boundary condition to simplify the calculation. Thus N is the number of planes in one unit cell and the boundary condition is

$$J_{l,l\pm1}=J_{N+l,N+l\pm1},\quad l=1,2,\ldots,N\ . \tag{18}$$

Since $J_{1,0}$ and $J_{L,L+1}$ are no longer zero, the hopping between the interface of the neighboring unit cells should be considered. Two more self-energy terms, which come from cycling diagrams in the counterclockwise and clockwise directions, respectively (see Appendix A), should be added. The solution then can be written as

$$\frac{1}{\hat{G}_{l,l}}=\frac{1}{\hat{G}^0_{l,l}}-\hat{\Sigma}^{UB}_l-\hat{\Sigma}^{DB}_l-\hat{\Sigma}^{UC}_l-\hat{\Sigma}^{DC}_l\ , \tag{19}$$

$$\hat{G}_{l,l'}=\hat{G}_{l,l}\prod_{i=1}^{i=l'-l}\hat{T}_{l+i-l,l+i}\hat{U}_l(l+i)+\hat{G}_{l,l}\prod_{i=1}^{i=N-l'+l}\hat{T}_{l-i+1,l-i}\hat{D}_l(l-i),\quad l<l'\ , \tag{20}$$

$$\hat{G}_{l,l'}=\hat{G}_{l,l}\prod_{i=1}^{i=l-l'}\hat{T}_{l-i+1,l-i}\hat{D}_l(l-i)+\hat{G}_{l,l}\prod_{i=1}^{i=N+l'-l}\hat{T}_{l+i-1,l+i}\hat{U}_l(l+i),\quad l>l'\ , \tag{21}$$

where $\hat{\Sigma}^{UC}_l$ and $\hat{\Sigma}^{DC}_l$ are defined through the matrices $\hat{U}$ and $\hat{D}$:

$$\hat{\Sigma}^{UC}_l=\left[\sum_{i=1}^{N-2}\hat{T}_{l+i-1,l+i}\cdot\hat{U}_l(l+i)\right]\hat{T}_{l-1,l}\ , \tag{22}$$

$$\hat{\Sigma}^{DC}_l=\left[\prod_{i=1}^{N-2}\hat{T}_{l-i+1,l-i}\cdot\hat{D}_l(l-i)\right]\hat{T}_{l+1,l}\ . \tag{23}$$

Here a modulus N is taken if the labels run out of the unit cell. The expressions for $\hat{\Sigma}^{UB}_l$ and $\hat{\Sigma}^{DB}_l$ are given in Eqs. (A5) and (A6). They are different from Eqs. (15) and (16) since the starting points of iteration are $l-1$ and $l+1$ instead of layer N or layer 1, respectively.

B. Charge-carrier transfer effect

The Fermi energy $E_F(l)=\mu_l$ at zero temperature could vary drastically from layer to layer in the SN junction and S/N superlattice if the density of the charge carrier in the normal layer is very low compared to that of the superconductor. In this case the charge-carrier transfer across the S/N interface may become important, which could result in a substantial change of the Fermi energy, especially in the normal layer. In order to study this effect, we adopt a semiclassical approach. The change of the charge-carrier density in the lth plane is defined as

$$\delta n(l)=\int_{U(l)}^{E_F}N_l dE-\int_0^{E_F(l)}N_l dE\ , \tag{24}$$

where $E_F(l)$ and E_F are the Fermi energy in the lth plane before and after the charge-carrier transfer. $U(l)$, the electrostatic potential shift due to $\delta n(l)$, can be solved by the Poisson equation in the form of the difference equation

$$U(l+1)-2U(l)+U(l-1)-\frac{4\pi e^2d^2\delta n(l)}{\epsilon(l)}=0\ , \tag{25}$$

self-consistently in combination with Eq. (24). Here d is the interlayer spacing, which is estimated as ~ 6 Å for Y-Ba-Cu-O. If we take a summation of Eq. (25) from $l=1$ to N, the following relation is obtained

$$\sum_{l=1}^{N}\delta n(l)=0\ , \tag{26}$$

which implies that the total change of the charge carriers within one unit cell is zero. For the finite multilayer, in order to satisfy the above conservation equation, the condition that the electrostatic field outside zero is applied,

$$U(N+1)=U(N),\quad U(0)=U(1)\ . \tag{27}$$

Therefore the total charge carrier is conserved during the charge-carrier transfer.

In Fig. 1 the relative change of the charge-carrier density $[\delta n(l)/n_0(l)]$ in the unit cell of a S/Sm superlattice is plotted for different N_s and N_m. Here $N_s+N_n=N$. The original charge-carrier densities for S and Sm are chosen to be $4\times10^{21}/\text{cm}^3$ and $1.0\times10^{19}\text{cm}^3$, respectively. It is obvious that the relative charge-carrier density change in the S layer is negligibly small (smaller than 1%) while that in N layer could be as large as 200%. Therefore any effect on T_c is unlikely induced dominantly by the charge-carrier transfer effect for the c-oriented S/N superlattice. It should be pointed out that this argument is based on the assumption that the electronic structure of each layer has not been changed, which is generally the case of c-oriented devices. For a-oriented devices,[21–23] when the thickness of the superconducting layer is comparable to the coherence length along the a axis, the electronic structure of the superconductor may

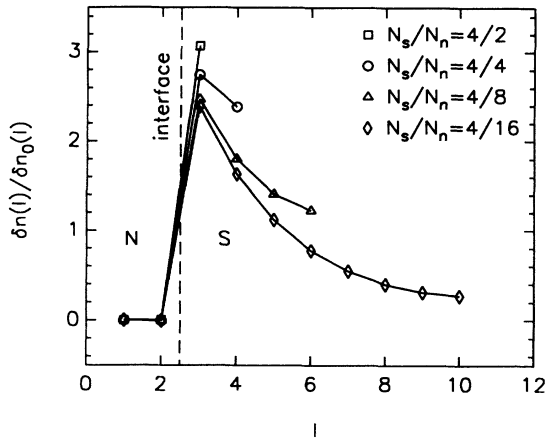

FIG. 1. Distribution of the relative charge-carrier transfer in a unit cell of the S/Sm superlattice.

already be dramatically modified so that the charge-carrier transfer effect could be important.

III. RESULT

With the solution of the Gor'kov equation, many physical properties of the superconducting layered structures can be discussed. In the following, the transition temperature of a S_1/S_2 and a S/Sm superlattice will be studied (Sec. III A). By investigating the proximity effect near the interface of the superconductor and normal material, especially by computing the coherence length ξ_s and the Cooper pair leaking length ξ_N, some physical insight has been obtained (Sec. III B).

A. Transition temperature

1. S_1/S_2 superlattices

If two different superconducting materials are deposited layer by layer alternatively, such as $YBa_2Cu_3O_7/DyBa_2Cu_3O_7$ superlattice[6] or Y-Ba-Cu-$O/Y_{1-x}Pr_xBa_2Cu_3O_7$ superlattice[24] when $X<0.5$, we call it S_1/S_2 superlattice. The formalism discussed in Sec. II for superlattice can be directly applied to this system. The distribution of the energy gap is described by

$$\Delta_l=2N_lV_lk_BT\int_0^{E_f(l)}d\xi_l\sum_{n=-\infty}^{\infty}F_{l,l}(\xi_l,\omega_n)\ ,$$
$$l=1,2,\ldots,N\ . \quad (28)$$

Here N_l is the density of state at the Fermi surface for the lth plane. The hopping matrix has the following form generally:

$$T_{l,l'}=\begin{cases}J_1\delta_{l,l\pm1}, & \text{inside } S_1\\ J_2\delta_{l,l\pm1}, & \text{inside } S_2\\ J_{12}\delta_{l,l\pm1}, & S_1 \text{ and } S_2 \text{ interface}\ .\end{cases} \quad (29)$$

When the temperature approaches the superconducting transition temperature T_c, the system will experience a second-order phase transition; therefore the order parameter or the energy gap Δ_l approaches zero. Thus we may assume that they are small quantities in the vicinity of T_c and linearize Eq. (28). T_c can then be solved from the nontrivial solution of this linearized equation:

$$\Delta_l-2N_lV_lk_BT\int_0^{E_f(l)}d\xi_l\sum_{n=-\infty}^{\infty}\sum_{l'}\left.\frac{\partial F_{l,l}(\xi_l,\omega_n)}{\partial\Delta_{l'}}\right|_{|\Delta_i|_s'=0}\Delta_{l'}=0,\quad l=1,2,\ldots,N\ . \quad (30)$$

In Fig. 2, the transition temperature T_{c12} of a S_1/S_2 superlattice with $N_{s1}=N_{s2}=2$ is shown for different hopping constants. Here we have taken $J=J_1=J_2=J_{12}$ for simplicity of the discussion. The transition temperature has been normalized to that of S_1 at $J_1=0$. In our calculations, we have chosen N_lV_l to be 0.39 and 0.34 for S_1 and S_2, respectively. The Fermi energies are assumed 0.127 eV for both S_1 and S_2 and the charge carrier transfer effect has been neglected because the difference of the charge-carrier density between these two superconductors is assumed little.

Curves T_{c1} and T_{c2} in Fig. 2 are the transition temperatures for layered structures composed of only S_1 or S_2, respectively. The transition temperature of the S_1/S_2 superlattice T_{c12} locates in between T_{c1} and T_{c2} because of the proximity effect,[25] i.e.,

$$T_{c1}>T_{c12}>T_{c2}\ . \quad (31)$$

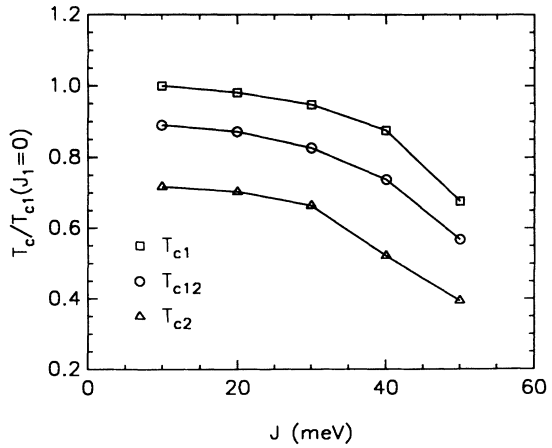

FIG. 2. Superconducting transition temperature in S_1 (T_{c1}), S_2 (T_{c2}), and S_1/S_2 (T_{c12}) superlattices.

We have also checked the transition temperature for the varying thickness of S_1 and found that T_{c12} will saturate to T_{c1} with increasing thickness of the S_1 layer, and vice versa. Our calculation also shows that T_c drops monotonically with increasing hopping constant because the break of the Cooper pairs during the charge hopping destroys the superconductivity.

2. *S/Sm superlattice*

If the superconductor and semiconductor or insulator are deposited alternatively, we have a *S/Sm* or *S/I* superlattice. Among them the Y-Ba-Cu-O/Pr-Ba-Cu-O superlattice is a popular one. Sine the coherence length of the HTS's is very short, the discussions for *S/Sm* and *S/I* superlattices are similar. Therefore we will consider only the *S/Sm* superlattice for simplicity.

An important difference between the S_1/S_2 and *S/Sm* superlattices is that the latter may not become superconducting at any temperature if the thickness of the normal layer is large compared to the coherence length of the superconductor.[26] In another words, a *S/Sm* superlattice may be composed of many superconducting islands separated by the normal layers which will not become superconducting due to the proximity effect. As we already know, the coherence length of Y-Ba-Cu-O is about 3–5 Å along the *c* direction, which is certainly not long enough to make Pr-Ba-Cu-O superconducting in the Y-Ba-Cu-O/Pr-Ba-Cu-O superlattices by the proximity effect because the thickness of the Pr-Ba-Cu-O layer is at least 12 Å. However, the charge-carrier transfer effect in the *S/Sm* interface may become substantial because the charge density of superconductor is estimated two to three orders higher than that of semiconductor. Therefore the regular method of calculating the transition temperature of a superconducting superlattice as it is discussed in Sec. III A 1 can no longer be applied here.

Based on this argument, the energy gap is no longer a proper order parameter in a *S/Sm* multilayer since the pair coupling in the semiconducting layers is zero. Instead solving the energy gaps by Eq. (28), we will calculate the pair amplitude $F_{l,l}(0,0)$ in each plane by the following equation:

$$F_{l,l}(0,0)=2N_l k_B T \int_0^{E_f-U(l)} d\xi_l \sum_{n=-\infty}^{\infty} F_{l,l}(\xi_l,\omega_n) ,$$
$$l=1,2,\ldots,N . \quad (32)$$

Due to the proximity effect, the superconducting pairs can leak into the semiconducting layers; therefore the pair amplitude in *Sm* is not zero and can be solved self-consistently. However, the transition temperature of a *S/Sm* superlattice cannot be obtained by linearizing the above equation because the superconducting phase transition in the *Sm* layer is senseless. Instead, we will find out T_c by calculating the temperature dependence of the pair amplitude. Below T_c, $F_{l,l}$ is finite and when $T=T_c$, $F_{l,l=0}$. It has been noticed that the integral limit of Eq. (32) is shifted from $(0,E_f(l))$ to $(0,E_f-U(l))$ by considering the charge-carrier transfer effect.

In Fig. 3 the transition temperature of a *S/Sm* superlattice has been plotted against the number of the *Sm* layer for $J=20$ and 30 meV and $Ns=2$ and 4, respectively. The density of state for *Sm* layer is estimated two orders lower than that of the *S* layer. It is interesting to see in Fig. 3 that the transition temperature of a *S/Sm* superlattice drops initially with increasing thickness of the *Sm* layer and then saturates to a finite value T_{cs} instead of going to zero. The saturation temperature T_{cs} increases with the thickness of the *S* layer which, as we will discuss in the next section, is compatible with coherence length in the *S* layer. When the superconductor is much thicker than the coherence length, T_{cs} will be less sensitive to the thickness of the *Sm* layer. The increase of the hopping constant will result in a decrease of T_{cs} and a bigger *Sm* thickness to reach the saturation because both the coherence length ξ_s in the *S* layer and the Cooper pair leaking length ξ_N are increasing with the hopping const (see Sec. III B). In Ref. 16, we have compared our calculations with the experimental result quantitatively and found that the agreement between theoretical and experimental results is very good under the parameter we chose. Therefore we would like to point out that the depression of the transition temperature in the Y-Ba-Cu-O/Pr-Ba-Cu-O superlattice is caused dominantly by the proximity effect. We believe that this saturation phenomenon is universal for a *c*-oriented HTS/*Sm* superlattice.

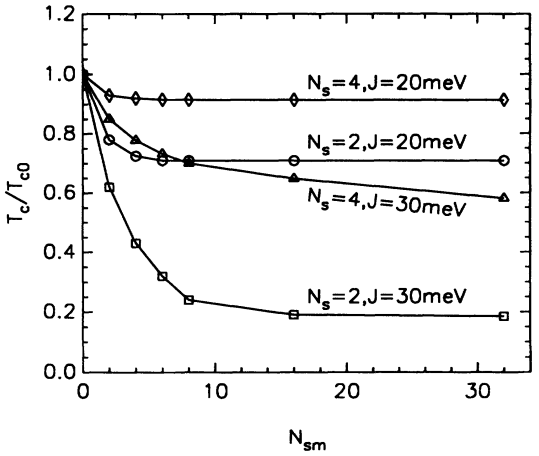

FIG. 3. Dependence of the normalized transition temperature on the thickness of the *Sm* layer.

B. Coherence length

In order to obtain some insight, we will calculate the coherence length in the superconducting layers and the Cooper pair leaking length in the semiconducting layers.

1. ξ_s *in superconductor*

The coherence length ξ_s can be obtained by calculating the off-diagonal term of the anomalous Green's function $F_{l,l'}(0,0)$.[18] Taking $N_s=20$ and $N_{sm}=14$ in the *S/Sm* superlattice, we can label the planes in a unit cell. Therefore planes 1–20 are from *S* and planes 21–34 are from *Sm*. $F_{l,l'}$ in *S* layers are then calculated with $l'=10$ and $l-l'=2,4,6,8,10$. Since $F_{l,l'}$ drops approximately ex-

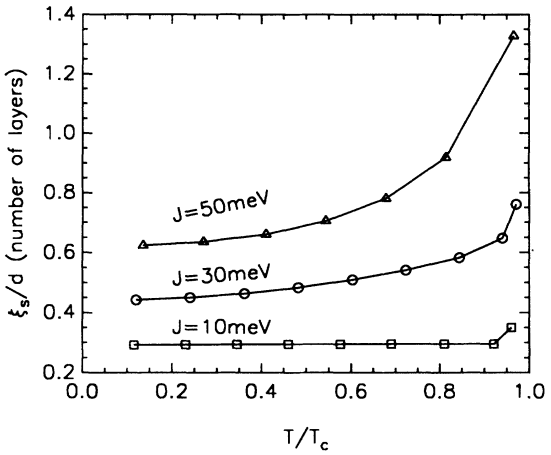

FIG. 4. Temperature dependence of the coherence length ξ_s.

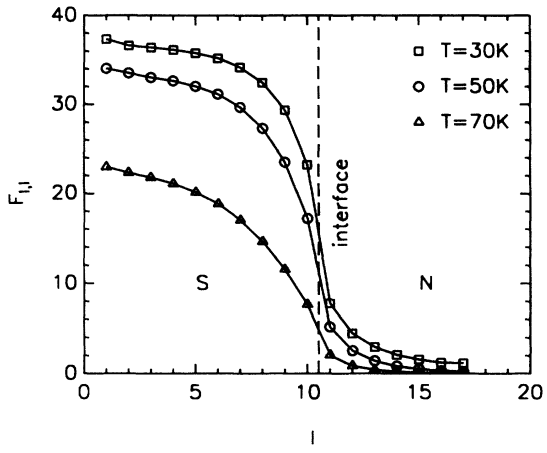

FIG. 5. Distribution of the pair amplitude across the interface of the superconductor and normal material at different temperatures.

ponentially with $l-l'$, we therefore calculated the coherence length by the following relation:[26]

$$F_{l,l'}(\mathbf{r},\tau)=\text{const. exp}\left[-\frac{l-l'}{\xi_s}\right] . \tag{33}$$

The coherence length thus calculated has been displayed as a function of the normalized temperature and the hopping constant in Fig. 4. It is interesting to see that within a wide temperature range below T_c, ξ_s is almost a constant. In Ref. 16, we have chosen $J=30$ meV to fit the measured T_c in the Y-Ba-Cu-O/Pr-Ba-Cu-O superlattice. The coherence length calculated in Fig. 4 at this value is about 0.4–0.8 inter–Cu-O plane spacing within the range $T/T_c<0.95$, i.e., 3–5 Å, which is consistent with the well-known experimental result for Y-Ba-Cu-O. Therefore, when the temperature is not very close to T_c, the charge-carrier pairing stays in the 2D type. In the vicinity of T_c, ξ_s increases sharply and approaches to infinity as $T\rightarrow T_c$, which implies charge-carrier hopping may help to form a weak interlayer pairing around T_c.

In the Y-Ba-Cu-O/Pr-Ba-Cu-O superlattices, when $N_s=2$, the Cooper pair in the Y-Ba-Cu-O layer has a comparable size with the layer thickness so that it is easy to be broken. Therefore the transition temperature of the superlattice is drastically depressed. This depression is then weakened as the thickness of the S layer is increased. It has been shown in Fig. 2 of Ref. 16 that $T_c/T_{c0}\sim 0.8$ when $N_s=8$ where the coherence length is very short compared to the thickness of the Y-Ba-Cu-O layer. The influence of the proximity effect on the deeper layer of Y-Ba-Cu-O from the interface is already screened out by the layer near the interface. With further increasing of the thickness of the Y-Ba-Cu-O, the transition temperature will saturate to T_{c0}, which is the transition temperature of the Y-Ba-Cu-O thin film.

2. *Cooper pair penetration length* ξ_N

In Fig. 5 we have shown how the pair amplitude $F_{l,l}$ drops across the interface from the superconductor to the normal layer. The layers 1–10 represent the superconductor while layers 11–17 are the semiconductor. As is shown in Fig. 5, the penetration of the Cooper pair into the N side increases with the hopping constant. The transition area across the interface is very sharp at low hopping constant and becomes broader as the hopping constant is increased. The distribution of $F_{l,l}$ can be fitted approximately by the following formula[26]

$$F_{l,l}\propto \exp\left[-\frac{l-l_0}{\xi_N}\right] . \tag{34}$$

In Fig. 6, ξ_N has been plotted as a function of $1/T$ for $J=10$, 30, and 50 meV. It has been noticed that all those curves can be described approximately by the equation

$$\xi_N=A(J)/T , \tag{35}$$

if the temperature is not very low. As T approaches T_c,

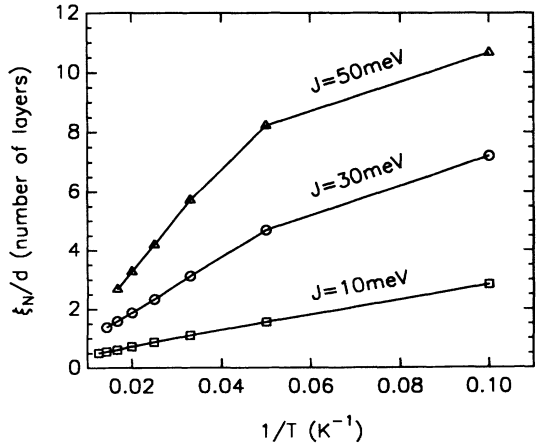

FIG. 6. Temperature dependence of the Cooper pair leaking length.

only a few Cooper pairs could survive and penetrate to the N side so that ξ_N is actually zero. This is obvious in Fig. 6 if the curves are extrapolated to the high-T end. $A(J)$ is a monotonic function of the hopping constant. This $1/T$ relation may suggest Pr-Ba-Cu-O is clean,[25] which is not difficult to accept because of the structure similarity between Y-Ba-Cu-O and Pr-Ba-Cu-O; the former has been known as a clean material.

Our calculations have shown here that the Cooper pair penetration length ξ_N is about two to three Cu-O plane spacing under the parameters in Ref. 16. It implies that the Cooper pairs can only enter very thin layers of the semiconductor. The deeper *Sm* layers stay in the normal state so that many superconducting islands centered at the superconductor are formed below the transition temperature of the superlattice. Therefore when the thickness of the *Sm* layer in the *S/Sm* superlattice is increased, the influence on T_c is actually saturated. Experimentally, we expect this T_c saturation if the coherence length is short compared to the thickness of the *S* and *Sm* layers.

IV. CONCLUSIONS AND DISCUSSIONS

In conclusion, we have established a general formalism to discuss the superconducting proximity effect in an inhomogeneous layered structure. The advantage of this formalism is obvious. First, since it is derived directly from the Gor'kov equation, certainly it can be used in the whole temperature range below T_c. Second, it can be applied to any inhomogeneous layered system, especially the HTS materials where the nonuniformity in a very short scale is inevitable. Third, in calculating the self energy, we have made the summation over all the possible connected Feynmman diagrams caused by the nearest-neighbor charge-carrier hopping so that solutions given in Eqs. (12), (13), and (19)–(21) are the exact solutions of the Gor'kov equation under the mean-field approximation even though the perturbation method has been adopted in the derivation.

Utilizing the established formalism, we have studied the proximity effect in the *S/N* interface and *S/N* superlattice. Several interesting results have been obtained. It has been found that the transition temperature of *S/Sm* superlattice will decrease and then saturate to a finite value with increasing thickness of *Sm* layer. The depression of T_c is large when the thickness of the *S* layer is compatible with the coherence length. The semiconducting layers will remain nonsuperconducting in the *S/Sm* superlattice since the Cooper pair leaking length ξ_N is small. Therefore the *S/Sm* superlattice is composed of many superconducting islands. Our calculations have explained most experimental features for the Y-Ba-Cu-O/Pr-Ba-Cu-O superlattices. The calculated inversely linear T dependence of ξ_N implies that our formalism can be applied directly to most normal materials in the clean limit.

Our formalism could be more useful under the following modifications. (1) The two-dimensional BCS-type pair coupling for the superconductivity can be extended to an anisotropic pair coupling (i.e., intralayer coupling plus interlayer coupling) if the interlayer coupling is limited within the unit cell. This assumption is not very rigorous because the 2D behavior has been observed for most HTS's if the temperature is not very close to T_c. On the other hand, since the *a*-oriented Y-Ba-Cu-O/Pr-Ba-Cu-O trilayers[21,22] and superlattice[23] have been reported, the inclusion of the interlayer pair coupling within several layers will be important to explain the experimental observations. (2) In this paper, only equilibrium properties have been discussed to keep this paper short. By introducing electrical and magnetic fields, the nonequilibrium properties can be studied. In particular, the linear response behavior when the fields are weak will be very important for the device applications of the HTSC materials. (3) We have adopted a coherent tunneling Hamiltonian in Eq. (1) which is based on the assumption that the number of the scattering centers along the *c* direction is not very large. The calculation of the incoherent tunneling is also possible even though it is a little complicated. At this moment, it is still too early to judge which one is dominant because of the lack of experimental data.

ACKNOWLEDGMENTS

We would like to thank Dr. J. R. Hu and Dr. Z. Y. Weng for helpful discussions. This work was supported by the Texas Center for Superconductivity at the University of Houston under the prime grant from DARPA and the State of Texas and a grant from the Robert A. Welch Foundation.

APPENDIX A

As we see from Eq. (7), the solution of the Green's function is actually equal to the inversion of the matrix $\hat{K}$. Assuming it is composed of a dominant diagonal term and a perturbative off-diagonal term (later on we will find this assumption is not necessary), i.e.,

$$\hat{K}=\hat{K}_0-\hat{K}' , \tag{A1}$$

we can expand the Green's function as a perturbative series

$$\hat{G}=(\hat{K}_0-\hat{K}')^{-1}=\hat{K}_0^{-1}\sum_{n=0}^{n=\infty}(\hat{K}'\hat{K}_0^{-1})^n . \tag{A2}$$

For each element of $\hat{G}$, the expansion is of the following form:

$$\hat{G}_{l,l'}=\hat{G}^0_{l,l}+\hat{G}^0_{l,l}\left[\hat{T}_{l,l'}+\sum_m \hat{T}_{l,m}\hat{G}^0_{m,m}\hat{T}_{m,l'}+\cdots+\sum_{m_1,m_2,\ldots,m_n} T_{l,m_1}\hat{G}^0_{m_1,m_1}\hat{T}_{m_1,m_2}\cdots\hat{G}^0_{m_n,m_n}\hat{T}_{m_n,l'}+\cdots\right]\hat{G}^0_{l',l'} . \tag{A3}$$

here $\hat{T}_{l,m}$ and $\hat{G}^0_{l,l}$ have been given in Eqs. (10) and (14), respectively. Since the solution of the superlattice is more complicated than that of the finite multilayer, in the following we will derive the solution of the superlattice first. At the end of this section, we will show that the solution of the finite multilayer can be obtained directly from our derivation.

If we look carefully at the expansion (A3), and assume that $\hat{G}^0_{m,m}$ represents site m and $\hat{T}_{n,m}$ acts as the bridge from site n to site m [see Fig. 7(a)], each term in the expansion can then be represented by a different diagram starting from layer l and ending at layer l'. The element $\hat{G}_{l,l'}$ is therefore a summation of all the different diagrams from l to l'. The weighting factor for each diagram is 1.

Let us first discuss the diagrams for the diagonal elements of the Green's function. Under the periodic boundary condition (18), the superlattice can be simplified to a unit cell with 1st and Nth connected to form a circle [see the third drawing in Fig. 7(a) for $N=4$]. Each diagram from l to l can then be decomposed into four types of basic units; we call them $\hat{\Sigma}^{UB}_l, \hat{\Sigma}^{DB}_l, \hat{\Sigma}^{UC}_l$ and $\hat{\Sigma}^{DC}_l$. The schematic representation of these four units has been given in Figs. 7(b)–7(e), respectively. Here the superscripts U and D are the abbreviations of down or up, which imply the directions of the first bridge from site l is to $l'<l$ or $l'>l$, respectively. B and C are the abbreviations of back and circle, which identify the way to build up the series of the bridges by going back or making a circle to site l.

In Figs. 7(b) and 7(c), we see the farthest sites from site l for $\hat{\Sigma}^{UB}_l$ and $\hat{\Sigma}^{DB}_l$ are, respectively, site $l-1$ and $l+1$. If we define $\hat{\Sigma}^{UB}_l(m)$ $(m>l)$ to be the total routes from site m up to site $l-1$ and then back to site m, $\hat{\Sigma}^{UB}_l(m-1)$ can then be obtained by adding site $m-1$ to $\hat{\Sigma}^{UB}_l(m)$, which is

$$\hat{\Sigma}^{UB}_l(m-1)=\hat{T}_{m-1,m}\sum_{n=0}^{n=\infty}[\hat{G}^0_{m,m}\hat{\Sigma}^{UB}_l(m)]^n\hat{G}^0_{m,m}\hat{T}_{m,m-1}\ , \tag{A4}$$

or

$$\hat{\Sigma}^{UB}_l(m-1)=\hat{T}_{m-1,m}\{(\hat{G}^0_{m,m})^{-1}-\hat{\Sigma}^{UB}_l(m)\}^{-1}\hat{T}_{m,m-1}\ . \tag{A5}$$

Similarly, the iterative equation for $\hat{\Sigma}^{DB}_l(m+1)$ is

$$\hat{\Sigma}^{DB}_l(m+1)=\hat{T}_{m+1,m}\{(\hat{G}^0_{m,m})^{-1}-\hat{\Sigma}^{DB}_l(m)\}^{-1}\hat{T}_{m,m+1}\ . \tag{A6}$$

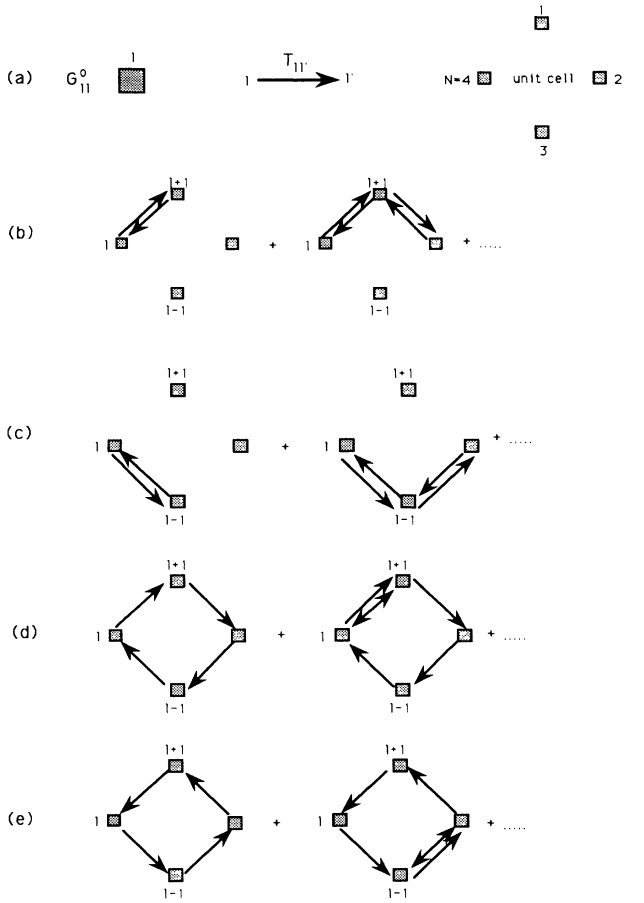

FIG. 7. (a) Definitions of the site and bridge; and the diagrammatic expressions of the self energies: (b) Σ^{UB}_l, (c) Σ^{DB}_l, (d) Σ^{UC}_l, and (e) Σ^{DC}_l.

Applying the boundary conditions

$$\hat{\Sigma}^{UB}_l(l-1)=0,\quad \hat{\Sigma}^{DB}_l(l+1)=0\ , \tag{A7}$$

we obtain $\hat{\Sigma}^{UB}_l=\hat{\Sigma}^{UB}_l(l)$ and $\hat{\Sigma}^{DB}_l=\hat{\Sigma}^{DB}_l(l)$ by the iteration relations (A5) and (A6), respectively.

With the help of $\hat{\Sigma}^{UB}_l$ and $\hat{\Sigma}^{DB}_l$, the cyclic diagrams $\hat{\Sigma}^{UC}_l$ and $\hat{\Sigma}^{DC}_l$ can be formed step by step through all the layers:

$$\hat{\Sigma}^{UC}_l=\hat{T}_{l,l+1}\hat{U}_l(l+1)\hat{T}_{l+1,l+2}\hat{U}_l(l+2)\cdots\hat{T}_{l-2,l-1}\hat{U}_l(l-1)\hat{T}_{l-1,l}\ , \tag{A8}$$

$$\hat{\Sigma}^{DC}_l=\hat{T}_{l,l-1}\hat{D}_l(l-1)\hat{T}_{l-1,l-2}\hat{D}_l(l-2)\cdots\hat{T}_{l+2,l+1}\hat{D}_l(l+1)\hat{T}_{l+1,l}\ . \tag{A9}$$

Here in order to shorten the writing, we have used the notation $\hat{U}_l(m)$ and $\hat{D}_l(m)$, which are defined as

$$\hat{U}_l(m)=[(\hat{G}^0_{m,m})^{-1}-\hat{\Sigma}^{UB}_l(m+1)]^{-1}\ , \tag{A10}$$

$$\hat{D}_l(m)=[(\hat{G}^0_{m,m})^{-1}-\hat{\Sigma}^{DB}_l(m-1)]^{-1}\ . \tag{A11}$$

Physically the difference between $\hat{\Sigma}^{UB}_l$ and $\hat{U}_l$ is clear. The former is the summation of all noncyclic connected

diagrams along the up direction and the latter, that including both connected and unconnected diagrams under the same condition. The explanations for $\hat{\Sigma}_l^{DB}$ and $\hat{D}_l$ are very similar. We would like to mention that when the diagrams pass through the superlattice unit-cell boundary, the modulus N for the layer number is taken simultaneously so that the equation for the Green's function is closed up within one unit cell of the superlattice. Since each diagram in the expansion of $\hat{G}_{l,l}$ can be formed by these four basic element diagrams, the solution for $\hat{G}_{l,l}$ can then be written as Eq. (19) (Ref. 18) following the basic rule of the Feynman diagram.

The off-diagonal element of the Green's function $\hat{G}_{l,l'}$ is the combination of diagrams from l to l and then l to l' (no longer going back to l). For the superlattice there are two possible directions to reach l'. For $l>l'$, one is directly going down from l to l' and the other is going up cyclically through $l+1,l+2,\ldots,l'-2,l'-1$, then to l'. That is,

$$\hat{G}_{l,l'}=\hat{G}_{l,l}\{\hat{T}_{l,l-1}\hat{D}_l(l-1)\cdots\hat{T}_{l'+1,l'}\hat{D}_l(l') +\hat{T}_{l,l+1}\hat{U}_l(l+1)\hat{T}_{l+1,l+2}\cdots\hat{T}_{l'-1,l'}\hat{U}_l(l')\}\ . \tag{A12}$$

Similarly we can write the solution for $\hat{G}_{l,l'}$ when $l<l'$,

$$\hat{G}_{l,l'}=\hat{G}_{l,l}\{\hat{T}_{l,l+1}\hat{U}_l(l+1)\cdots\hat{T}_{l'-1,l'}\hat{U}_l(l') +\hat{T}_{l,l-1}\hat{D}_l(l-1)\hat{T}_{l-1,l-2}\cdots\hat{T}_{l'+1,l'}\hat{D}_l(l')\}\ . \tag{A13}$$

The solution of the finite n layer is easy to obtain from the above derivation by simply applying the boundary condition (11). Equations (A5) and (A6) will start from $m=N$ and $m=1$, respectively, because $\hat{\Sigma}_l^{UB}(N)$ and $\hat{\Sigma}_l^{DB}(1)$ are zero. If we notice that $\hat{\Sigma}_l^{UB}(m)=\hat{\Sigma}_m^{UB}(m)$, Eqs. (A5) and (A6) can then be reduced to Eqs. (15) and (16), respectively. It is obvious that there is no cyclic diagram so that $\hat{\Sigma}_l^{UC}$ and $\hat{\Sigma}_l^{DC}$ are zero and only the first term in Eqs. (A12) and (A13) are left for the off-diagonal solution.

APPENDIX B

In deriving the solution of Eq. (7), we have used the perturbation method by assuming the off-diagonal elements are small compared to the diagonal elements. This assumption is actually not necessary since all the perturbative terms have been added up. Nevertheless it is necessary to give a rigorous proof that the solution we derived in Appendix A is the solution of Eq. (7).

In a matrix element form, Eq. (7) can be written as

$$\hat{G}_{l,l'-1}\hat{K}_{l'-1,l'}+\hat{G}_{l,l'}\hat{K}_{l',l'}+\hat{G}_{l,l'+1}\hat{K}_{l'+1,l'}=\hat{\delta}_{l,l'}\ . \tag{B1}$$

When $l=l'$, we can substitute the expressions of $\hat{G}_{l,l-1}$, $\hat{G}_{l,l}$ and $\hat{G}_{l,l+1}$ into Eq. (B1):

$$\hat{G}_{l,l}\{[\hat{T}_{l,l-1}\hat{D}_l(l-1)+\hat{T}_{l,l+1}\hat{U}_l(l+1)\cdots\hat{T}_{l-2,l-1}\hat{U}_l(l-1)]\hat{K}_{l-1,l}+\hat{K}_{l,l} +[\hat{T}_{l,l+1}\hat{U}_l(l+1)+\hat{T}_{l,l-1}\hat{D}_l(l-1)\cdots\hat{T}_{l+2,l+1}\hat{D}_l(l+1)]\hat{K}_{l+1,l}\}=\hat{I}\ . \tag{B2}$$

Using definitions (9) and (14) for $\hat{K}_{l,l\pm1}$ and $\hat{K}_{l,l}$ and multiplying the $\hat{G}_{l,l}^{-1}$ from the left, Eq. (B2) is reduced to

$$-\hat{T}_{l,l-1}\hat{D}_l(l-1)\hat{T}_{l-1,l}-\hat{T}_{l,l+1}\hat{U}_l(l+1)\cdots\hat{T}_{l-2,l-1}\hat{U}_l(l-1)\hat{T}_{l-1,l}+(\hat{G}_{l,l}^0)^{-1} -\hat{T}_{l,l+1}\hat{U}_l(l+1)\hat{T}_{l+1,l}-\hat{T}_{l,l-1}\hat{D}_l(l-1)\cdots\hat{T}_{l+2,l+1}\hat{D}_l(l+1)\hat{T}_{l+1,l}=(\hat{G}_{l,l})^{-1}\ . \tag{B3}$$

Comparing Eq. (B3) with Eqs. (A5), (A6), (A8), and (A9), we can immediately find that it is exactly the same as Eq. (19); therefore the diagonal elements of the solution satisfy the original equation (7). The proof for $l'=l\pm1$ is similar to that above; we leave it for readers to save the space here.

For $l>l'$ and $l'\neq l\pm1$, we substitute Eqs. (20) and (21) into Eq. (B1),

$$-\hat{G}_{l,l}\{\hat{T}_{l,l-1}\hat{D}_l(l-1)\hat{T}_{l-1,l-2}\cdots\hat{T}_{l',l'-1}\hat{D}_l(l'-1)\hat{T}_{l'-1,l'}+\hat{T}_{l,l+1}\hat{U}_l(l+1)\hat{T}_{l+1,l+2}\cdots\hat{T}_{l'-2,l'-1}\hat{U}_l(l'-1)\hat{T}_{l'-1,l'} -\hat{T}_{l,l-1}\hat{D}_l(l-1)\hat{T}_{l-1,l-2}\cdots\hat{T}_{l'+1,l'}\hat{D}_l(l')(\hat{G}_{l',l'}^0)^{-1}-\hat{T}_{l,l+1}\hat{U}_l(l+1)\hat{T}_{l+1,l+2}\cdots\hat{T}_{l'-1,l'}\hat{U}_l(l')(\hat{G}_{l',l'}^0)^{-1} +\hat{T}_{l,l-1}\hat{D}_l(l-1)\hat{T}_{l-1,l-2}\cdots\hat{T}_{l'+2,l'+1}\hat{D}_l(l'+1)\hat{T}_{l'+1,l'} +\hat{T}_{l,l+1}\hat{U}_l(l+1)\hat{T}_{l+1,l+2}\cdots\hat{T}_{l',l'+1}\hat{U}_l(l'+1)\hat{T}_{l'+1,l'}\}=0\ . \tag{B4}$$

We can separate the six terms on the left-hand side of Eq. (B4) into two groups. The three odd number terms can be written as follows:

$$-\hat{G}_{l,l}\hat{T}_{l,l-1}\hat{D}_l(l-1)\cdots\hat{T}_{l'+2,l'+1}\hat{D}_l(l'+1)\hat{T}_{l'+1,l'}\{\hat{I}-\hat{D}_l(l')[(\hat{G}_{l',l'}^0)^{-1}-\hat{T}_{l',l'-1}\hat{D}_l(l'-1)\hat{T}_{l'-1,l'}]\}\ . \tag{B5}$$

Recalling the definition for $\hat{D}_l(l')$ in Eq. (A10), the summation inside the brace of Eq. (B4) is actually zero. In a similar way, we can prove the three even-number terms contribute nothing to Eq. (B4) by using definition (A11). Therefore we have verified that Eqs. (19)–(21) are the solution of Eq. (7). The rigorous proof of the finite multilayer solution Eqs. (12) and (13) are very similar, so we will not give it here to keep this paper short.

*Permanent address: Department of Physics, Nanjing University, Nanjing, People's Republic of China.

[1]Y. Iye, in *Strong Correlations and Superconductivity,* edited by H. Fukuyama, S. Maekawa, and A. P. Malozemoff (Springer, Berlin, 1989).
[2]J. Z. Wu *et al.*, Phys. Rev. B **44**, 12 643 (1991).
[3]T. T. M. Palstra *et al.*, Phys. Rev. B **38**, 5102 (1988).
[4]C. Uher, J. Superconduct. **3**, 337 (1990).
[5]J. M. Triscone *et al.*, Phys. Rev. Lett. **64**, 804 (1990); Q. Li *et al.*, *ibid.* **65**, 1160 (1990).
[6]J. M. Triscone *et al.*, Phys. Rev. Lett. **63**, 1016 (1989).
[7]O. Nakamura *et al.*, Physica C **185**, 2069 (1991).
[8]C. T. Rogers *et al.*, Appl. Phys. Lett. **55**, 2032 (1989).
[9]H. Akoh *et al.*, Jpn. J. Appl. Phys. **27**, L519 (1988).
[10]U. Kabasawa *et al.*, Jpn. J. Appl. Phys. **29**, L86 (1990).
[11]X. X. Xi *et al.*, Appl. Phys. Lett. **59**, 3470 (1991).
[12]J. Mannhart *et al.*, Phys. Rev. Lett. **67**, 2099 (1991).
[13]W. L. McMillan, Phys. Rev. **175**, 537 (1968).
[14]Zs. Gulacsi, M. Gulácsi, and I. Pop, Phys. Rev. B **37**, 2247 (1988).
[15]T. Schneider and D. Baeriswyl, Z. Phys. B **73**, 5 (1988).
[16]J. Z. Wu *et al.*, Phys. Rev. B **44**, 411 (1991).
[17]S. Valdlamannati *et al.* (unpublished).
[18]J. R. Schrieffer, *Theory of Superconductivity* (Benjamin, New York, 1983).
[19]G. D. Mahan, *Many-Particle Physics* (Plenum, New York, 1981).
[20]K. S. Dy, S. Y. Wu, and T. Spratlin, Phys. Rev. B **20**, 4237 (1979).
[21]J. B. Barner *et al.*, Appl. Phys. Lett. **59**, 742 (1991).
[22]C. B. Eom *et al.*, Science **251**, 780 (1991).
[23]T. Hashimoto *et al.*, Appl. Phys. Lett. **60**, 1756 (1992).
[24]T. Venkatesan *et al.*, Appl. Phys. Lett. **56**, 391 (1990).
[25]G. Deutsher and P. G. de Gennes, in *Superconductivity,* edited by R. D. Parks (Dekker, New York, 1969).
[26]P. G. De Gennes, *Superconductivity of Metals and Alloys* (Benjamin, New York, 1966).

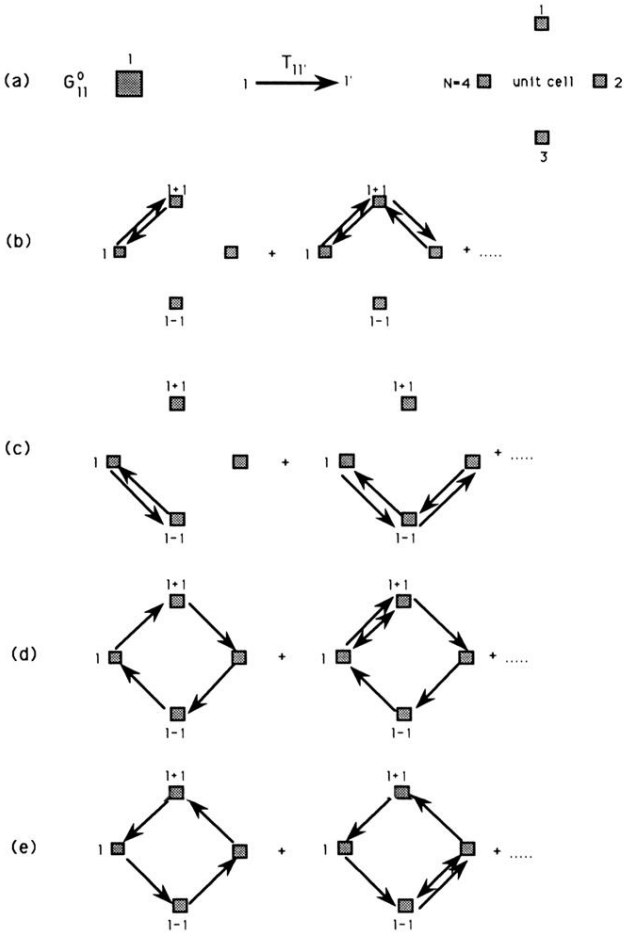

FIG. 7. (a) Definitions of the site and bridge; and the diagrammatic expressions of the self energies: (b) Σ_l^{UB}, (c) Σ_l^{DB}, (d) Σ_l^{UC}, and (e) Σ_l^{DC}.